Capillary Smectization and Layering in a Confined Liquid Crystal

D. de las Heras
Departamento de Física Teórica de la Materia Condensada, Universidad Autónoma de Madrid, E-28049 Madrid, Spain

E. Velasco
Departamento de Física Teórica de la Materia Condensada and Instituto de Ciencia de Materiales Nicolás Cabrera, Universidad Autónoma de Madrid, E-28049 Madrid, Spain

L. Mederos
Instituto de Ciencia de Materiales, Consejo Superior de Investigaciones Científicas, E-28049 Cantoblanco, Madrid, Spain
(Received 1 September 2004; published 6 January 2005)

Using density-functional theory, we have analyzed the phase behavior of a model liquid crystal confined between two parallel, planar surfaces (i.e., the so-called slit pore). As a result of confinement, a rich phase behavior arises. The complete liquid-crystal phase diagram of the confined fluid is mapped out as a function of wall separation and chemical potential. Strong commensuration effects in the film with respect to wall separation lead to enhanced smectic ordering, which gives *capillary smectization* (i.e., formation of a smectic phase in the pore), or frustrated smectic ordering, which suppresses capillary smectization. These effects also produce layering transitions. Our nonlocal density-functional-based analysis provides a unified picture of all the above phenomena.

DOI: 10.1103/PhysRevLett.94.017801 PACS numbers: 61.30.Hn, 64.70.Md, 68.15.+e

Liquid crystals confined in narrow pores have attracted considerable interest because of the profound effect of confinement on the phase behavior and dynamic properties of the material [1]. However, most experimental studies have focused on nematic materials and the search for the capillary nematization transition [2], with less attention being paid to the positionally ordered smectic phases, which have been analyzed in silica aerogels [3,4], controlled-pore glasses [5], and more recently using atomic-force microscopy [6]. From the theoretical perspective, recent advances have been based on microscopic theories, generally of the density-functional type [7], and computer simulations, in an effort to describe the properties of confined nematic materials, i.e., the phenomenon of capillary nematization and related wetting effects. Again, smectic phases have received little [8] or no attention whatsoever, mainly because of the lack of microscopic theories suitable for the highly inhomogeneous structures typical of genuine smectic ordering, even though some mesoscopic models have been applied to study the effect of positional ordering on the forces between surfaces confining the fluid [9]. Simulation studies have focused only on structural issues [10–13].

In this Letter, we investigate smectic ordering in a planar capillary (slit pore) using density-functional theory. We find that positional ordering and the interplay with confinement can give rise to a variety of layering phenomena. In particular, commensuration effects due to confinement produce a strong dependence of the phase diagram on the pore width. We also analyze how layering transitions are connected with the capillary nematic-smectic transition which occurs in a confined geometry. Our main finding is that the *capillary smectization* line (i.e., the continuation of the bulk nematic-smectic transition line when the fluid is confined) is not a single, connected line but a broken one; the resulting segments are intimately associated with the layering transitions that occur in the regime of complete wetting by smectic. Some of these effects have been found in other systems; our analysis provides a unified picture of all the above phenomena in model liquid crystals. Our findings are related to recent experimental studies of adsorbed smectic films using atomic-force microscopy [6] and provide what we believe are novel predictions that could be checked experimentally with the current experimental techniques.

We use a version of density-functional theory as applied to a hard-spherocylinder (HSPC) model for the interparticle interactions. The excess free energy is

$$\Delta F[\rho] = \int d\mathbf{r} d\mathbf{\Omega} \rho(\mathbf{r}, \mathbf{\Omega}) \Psi(\bar{\rho}_i) \int d\mathbf{r}' d\mathbf{\Omega}' \rho(\mathbf{r}', \mathbf{\Omega}') \times V(\mathbf{r} - \mathbf{r}', \mathbf{\Omega}, \mathbf{\Omega}'), \quad (1)$$

where V is the overlap function, ρ is the one-particle distribution function, and $\bar{\rho}_i$ are appropriately defined weighted densities (see details in Refs. [14–16]). The walls have been chosen to be identical, act as hard walls but only on the particles' centers of mass, and induce homeotropic alignment (see [17,18]). The local version of the theory was used previously [17,18] to investigate the wetting and confinement properties of the HSPC model on simple substrates: a rich phenomenology results in the phase behavior of the film which depends very strongly on the wetting properties of the system. However, the local nature of the theory prevented the global exploration of highly inhomogeneous structures inside the capillary, in particular, the occurrence of layered phases and the associated

commensuration effects. In this work, we choose the length (L)-to-breadth (D) ratio of the particles to be $L/D = 5$, which gives (athermal) isotropic $\leftrightarrow$ nematic $\leftrightarrow$ smectic-A liquid-crystal phase transitions as the chemical potential μ or mean density ρ_0 is increased [19,20].

Our main findings are represented in Fig. 1, which is the phase diagram of the confined fluid in the μ (chemical potential)-H (pore width) plane. The lines are only schematic—Fig. 3 contains real data corresponding to some selected regions of the phase diagram. We first focus on the regime of very wide pores. Layering transitions between phases with n smectic layers (S_n) and $n + 1$ smectic layers (S_{n+1}) occur by varying the pore width. These transitions are of first order. Also, a ''wavy'' *capillary smectization* line, located almost horizontally but with a small average slope such that $\mu \to \mu_{NS}$ as $H \to \infty$, separates confined phases, which we can term ''nematic'' (N), from phases that present smectic layers (S). This is the analogue of the capillary nematization transition occurring in a pore filled with an isotropic phase (I), also represented in the diagram. An important difference, however, is that the S phase presents a layered structure. Consequently, commensurability between the equilibrium smectic spacing and the pore width will necessarily lead to interference effects. These effects, which underlie the layering transitions in the S region, lead alternatively to frustration and enhancement of the smectic structure as H is varied and provide a mechanism to explain why layering and capillarity are intimately related. In fact, the two sets of coexistence lines meet at a series of triple points where three phases, N, S_n, and S_{n+1}, coexist. For narrow pores, however, this structure becomes disconnected. This phenomenon can be explained in terms of elastic effects associated with the layer compressibility B of the smectic structure. As H is varied for a structure with a fixed number of layers, S_n, the system builds an elastic energy since the layer spacing differs from the one in equilibrium. When this energy, $\sim B d_0$ (where d_0 is the equilibrium layer spacing), exceeds that needed to create a nematic structure in the center of the film, $\sim 2\gamma_{SN}$, the triple points will disappear (here γ_{SN} is the smectic-nematic surface tension). Our estimates for $B = 12.98 kT\sigma^{-1}$, $d_0 = 3.06\sigma$, and $\gamma_{SN} = 0.036 kT\sigma^{-2}$ (k being the Boltzmann constant, T the temperature, and σ an effective hard-sphere particle diameter such that $L + D = 2.93\sigma$; see [16] for details) give $n \sim 100$ as the number of layers where the triple point disappears and the N and S_{n+1} phases can be smoothly connected (i.e., without an intervening phase transition).

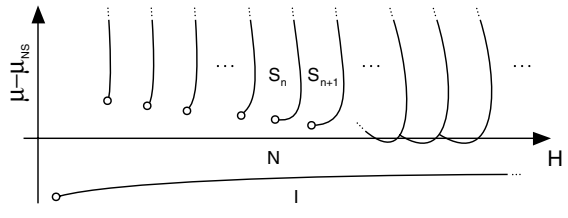

FIG. 1. Schematic phase diagram in the μ-H plane. μ_{NS} is the chemical potential at bulk N-S coexistence. At low H, coexistence lines are single lines terminating at critical points and separating phases with different structure. As H increases, the lines develop two regimes. At high H these lines meet and form triple points. N: nematic phase; S_n: ''smectic'' structure with n layers.

For lower H the phase-boundary lines have a double structure: a rather vertical sector, reminiscent of the layering transitions at high H, and a quite horizontal sector which corresponds to the broken capillary smectization transition. The latter is then broken into a number of segments or ''pockets'' terminating at critical points. The boundary lines cease to exist for the S_{10}-S_{11} transition and below; this feature is probably very prone to details of the theoretical model, but that the corresponding n should be roughly equal to 10 can be understood as follows. At coexistence the phases S_n and S_{n+1} have the same value of the grand potential for the same value of H. Clearly this is not the optimum value of H for both structures (with respect to the equilibrium layer spacing d in the bulk material). The S_{n+1} structure will stand up a point where $H = n(L + D)$. Since for HSPC's $d \simeq L + D$, and assuming that the maximum expansion of the layer spacing for the S_n phase is $d\Delta$, we should have $H = n(L + D) \leq (n - 1)(d + d\Delta) \simeq (n - 1)(1 + \Delta)(L + D)$, and we obtain $n \geq (1 + \Delta)/\Delta$. In order to have $n = 10$ we need $\Delta \simeq 0.1$, which appears as a reasonable value.

Figure 2 contains a set of density (ρ) and order-parameter ($\eta = \langle P_2(\cos\theta)\rangle$, where θ is the angle between the long axis of the particle and the director) profiles (only half of the profiles are shown; in all cases the wall is at the left). In the upper part, profiles corresponding to structures coexisting on the S_{27}-S_{26} transition line are shown. Note that they correspond to smectic structures with well-developed layers. The lower profiles correspond to coexisting structures with smectic (top) and nematic (bottom) character. In the latter case the order generated at the wall decays rather slowly to an almost constant value at the center of the pore.

Another interesting feature of the phase diagram is the existence of reentrant phases. As can be seen in Fig. 3(b), the vertical lines do in fact exhibit a change in slope, corresponding to a reentrant phase (this feature is common to all transitions, not just to the one shown). These transitions take place regardless of whether the transition lines are connected. In the case where the N and S phases are connected (i.e., there is no phase transition between the N and the S_{n+1} phases) the first transition is related to capillary smectization, $N \to S_n$, whereby the confined smectic phase appears at a lower chemical potential than in bulk. The second is a layering transition, $S_n \to S_{n+1}$, which may occur either at constant μ or at constant H. In the former case as the pore width is increased the system gets enough space to introduce one more layer, while in the latter as μ is increased the system reaccommodates by creating an additional layer. In the case where the N and S phases are

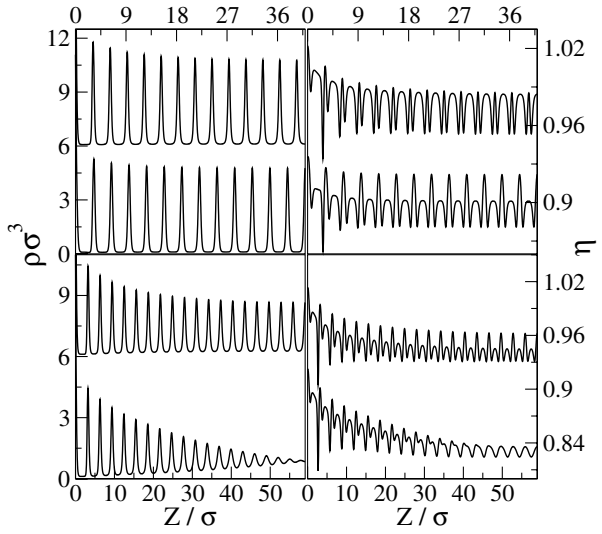

FIG. 2. Density (left side), $\rho\sigma^3$, and order-parameter (right side), η, profiles of coexisting phases. Upper diagrams: S_{27} (top) and S_{26} (bottom) phases at $\mu = 22.97kT$. Lower diagrams: S_{38} (top) and N (bottom) phases at $\mu = 21.61kT$. Only the left half of the profiles is shown (so that the right side of each diagram is at the center of the pore). Also, in each diagram the top profile has been shifted for the sake of clarity (6 units in density and 0.09 in order parameter).

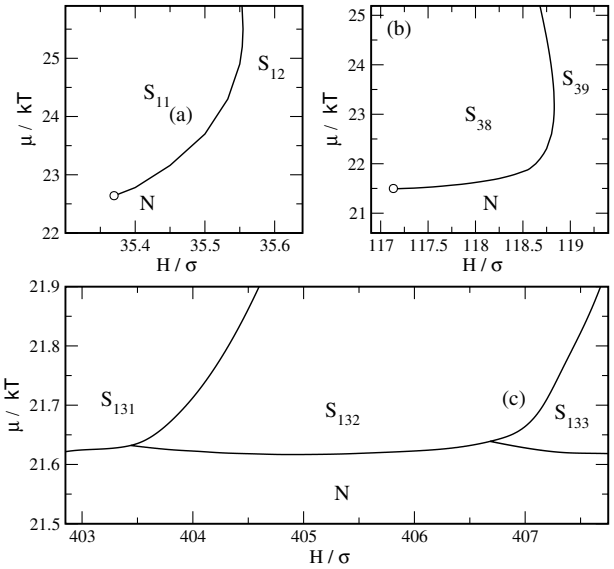

FIG. 3. Selected regions of the phase diagram in the μ-H plane. (a) S_{11}-S_{12} transition. (b) $S_{38} - S_{39}$ transition. (c) Layering transitions S_{131}-S_{132}-S_{133} and the capillary smectization transition N-S. Open circles indicate critical points.

not connected the two transitions reflect a truly reentrant smectic structure.

An interesting question is whether confinement reduces or increases the chemical potential $\mu(H)$ at which smectization occurs. An analysis based on the macroscopic Kelvin equation relates this problem to the wetting properties of the phase that nucleates inside the pore, $\mu(H) - \mu_{NS} = (\gamma_{\mathrm{WS}} - \gamma_{\mathrm{WN}})/[(\rho_S - \rho_N)H]$, $H \to \infty$ where the γ's are the surface tensions of the respective interfaces (WS: wall smectic; WN: wall nematic) and ρ_S and ρ_N are the number densities of the bulk smectic and nematic phases, respectively. Our estimates for the different surface tensions of the present model, $\gamma_{\mathrm{WS}}\sigma^2 = -14.155(30)kT$, $\gamma_{\mathrm{WN}}\sigma^2 = -14.125(1)kT$, and $\gamma_{NS}\sigma^2 = 0.036(1)kT$, correspond to $\Delta\gamma = \gamma_{\mathrm{WS}} + \gamma_{NS} - \gamma_{\mathrm{WN}} = 0.006(15)kT\sigma^{-2}$. Our present accuracy does not allow us to ascertain whether the smectic wets the substrate ($\Delta\gamma < 0$) or not ($\Delta\gamma > 0$). In any case the system should be close to a wetting condition, and this result is compatible with the results of Fig. 3 and the schematic representation in Fig. 1, which show that, in the regime of very wide pores, where the Kelvin equation should apply, the NS capillary line is slightly below the bulk chemical potential $\mu_{NS} = 21.636kT$, to which it tends as $H \to \infty$.

Experiments probing the effect of confinement on the nematic-smectic transition have been made on silica aerogels [3,4] which indicate a suppression of this transition. Recently, Kocevar and Musevic [6] have presented atomic-force microscopy (AFM) experiments where a confined 8CB liquid crystal in isotropic bulk conditions is studied in very narrow pores formed by one (planar) substrate and the (effectively planar) surface of a glass sphere attached to the AFM cantilever; this is closer to our model system than that on silica aerogels [4] where a random dispersion of pores introduces a high degree of disorder. The AFM experiments probe only conditions a few degrees centigrade above the bulk nematic-isotropic transition, i.e., with isotropic conditions in bulk. Oscillatory solvation forces have been observed, with increasing amplitude as the bulk nematic-isotropic (NI) transition is approached, indicating the presence of strong layering in the pore. Our solvation-force calculations (see Fig. 4) have been done in the regime of high chemical potential. The solvation force f_s shows a very strong and long-ranged oscillatory behavior with discontinuities signaling layering transitions as the corresponding transition lines are crossed. We are sweeping a region where there are no transitions for small H, hence the smooth behavior, but for wider pores there are discontinuities associated with layering and capillary smectization transitions (further results on the solvation forces near to the nematic-isotropic transition, a region explored by the AFM experiments [6], and its relation to the wetting properties of the material, can be found elsewhere [21]). These predictions should be confirmed by AFM measurements probing the low-temperature regime $T < T_{NI}$ and by calorimetric studies.

To summarize, we have investigated the phase behavior of a confined model liquid crystal that exhibits nematic and smectic bulk phases by means of a nonlocal density-functional theory. Confinement brings about capillary nematization and smectization transitions that occur at conditions of saturation different from those in the bulk. Our density-functional analysis indicates that there are

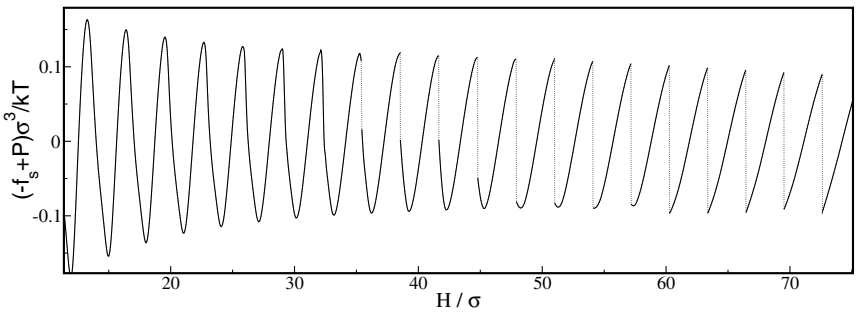

FIG. 4. Solvation force f_s as a function of pore width H for $\mu = 23.0kT$, $P = 13.90kT\sigma^{-3}$. The pressure P has been added to $-f_s$.

interesting commensuration effects that underlie both layering transitions and capillary smectization transitions. As the pore width is reduced the capillary smectization transition is broken up into pockets that terminate in surface critical points. The associated lines are in fact the coexistence lines corresponding to layering transitions between smectic structures of a different number of layers.

The physical system that we have analyzed is conceptually similar to the situation in a confined simple fluid. The latter was initially studied in Ref. [22] using a discrete $s = 1$-Ising model on a lattice. The bulk model contained three phases, which were identified as vapor, liquid, and solid, and strong commensuration effects gave rise to a complicated phase diagram with a strong oscillatory dependence with the pore width. Subsequent theoretical and simulation studies have confirmed this phenomenology. In our liquid-crystalline fluid we also have three phases, isotropic, nematic, and smectic, but two types of order, viz., orientational and positional, are involved.

Another question is how the layering transitions proceeding to higher chemical potentials terminate. Presumably, they will merge with a crystallization transition occurring in the confined system. Since the HSPC model has a considerable region where the smectic phase is stable prior to crystallization, we believe the structures and phase transitions shown in this work will survive in some range of chemical potential.

This work has been partly financed by the Spanish Ministry of Science and Technology under Grants No. BFM2001-0224-C02-01, No. BFM2001-0224-C02-02, and No. BFM2001-1679-C03-02. D. de las H. is supported by a FPU grant from the Spanish Ministry of Education and Culture.

[1] See, e.g., L. D. Gelb, K. E. Gubbins, R. Radhakrishnan, and M. Sliwinska-Bartkowiak, Rep. Prog. Phys. **62**, 1573 (1999).
[2] K. Kocevar, A. Borstnik, I. Musevic, and S. Zumer, Phys. Rev. Lett. **86**, 5914 (2001), and references therein.
[3] L. Wu, B. Zhou, C. W. Garland, T. Bellini, and D. W. Schaefer, Phys. Rev. E **51**, 2157 (1995).
[4] N. A. Clark, T. Bellini, R. M. Malzbender, B. N. Thomas, A. G. Rappaport, C. D. Muzny, D. W. Schaefer, and L. Hrubesh, Phys. Rev. Lett. **71**, 3505 (1993).
[5] Z. Kutnjak, S. Kralj, G. Lahajnar, and S. Zumer, Phys. Rev. E **68**, 021705 (2003).
[6] K. Kocevar and I. Musevic, Phys. Rev. E **65**, 021703 (2002).
[7] P. I. C. Teixeira, Phys. Rev. E **55**, 2876 (1997); R. van Roij, M. Dijkstra, and R. Evans, Europhys. Lett. **49**, 350 (2000); I. Rodriguez-Ponce, J. M. Romero-Enrique, E. Velasco, L. Mederos, and L. F. Rull, J. Phys. Condens. Matter **12**, A363 (2000); A. Chrzanowska, P. I. C. Teixeira, H. Ehrentraut, and D. J. Cleaver, J. Phys. Condens. Matter **13**, 4715 (2001); I. Rodriguez-Ponce, J. M. Romero-Enrique, and L. F. Rull, Phys. Rev. E **64**, 051704 (2001).
[8] For studies on related phenomenology, see V. Babin, A. Ciach, and M. Tasinkevych, J. Chem. Phys. **114**, 9585 (2001); T. Geisinger, M. Muller, and K. Binder, J. Chem. Phys. **111**, 5241 (1999).
[9] P. G. de Gennes, Langmuir **6**, 1448 (1990).
[10] M. P. Allen, J. Chem. Phys. **112**, 5447 (2000); J. Quintana, E. C. Poire, H. Dominguez, and J. Alejandre, Mol. Phys. **100**, 2597 (2002).
[11] R. E. Webster, N. J. Mottram, and D. J. Cleaver, Phys. Rev. E **68**, 021706 (2003).
[12] T. Gruhn and M. Schoen, J. Chem. Phys. **108**, 9124 (1998).
[13] H. Steuer, S. Hess, and M. Schoen, Phys. Rev. E **69**, 031708 (2004).
[14] A. M. Somoza and P. Tarazona, Phys. Rev. Lett. **61**, 2566 (1988).
[15] A. M. Somoza and P. Tarazona, Phys. Rev. A **41**, 965 (1990).
[16] E. Velasco, L. Mederos, and D. E. Sullivan, Phys. Rev. E **62**, 3708 (2000).
[17] D. de las Heras, E. Velasco, and L. Mederos, J. Chem. Phys. **120**, 4949 (2004).
[18] D. de las Heras, L. Mederos, and E. Velasco, Phys. Rev. E **68**, 031709 (2003).
[19] J. A. C. Veerman and D. Frenkel, Phys. Rev. A **41**, 3237 (1990).
[20] P. Bolhuis and D. Frenkel, J. Chem. Phys. **106**, 666 (1997).
[21] D. de las Heras, E. Velasco, and L. Mederos (unpublished).
[22] G. Navascués and P. Tarazona, Mol. Phys. **62**, 497 (1987).